MOCVD of $CoAl_2O_4$ Thin Films from $\{Co[Al(O^iC_3H_7)_4]_2\}$ as Precursor

N. El Habra,† L. Crociani,† C. Sada,§ P. Zanella,*,† M. Casarin,*,‡ G. Rossetto,†
G. Carta,† and G. Paolucci||

Istituto di Chimica Inorganica e delle Superfici (ICIS)−*CNR, Corso Stati Uniti 4, 35127 Padova, Italy,*
Dipartimento di Fisica, Università degli Studi di Padova, Via Marzolo 8, 35131 Padova, Italy,
Dipartimento di Scienze Chimiche, Università degli Studi di Padova, Via Loredan 4, 35131 Padova, Italy,
and Dipartimento di Chimica, Università Ca' Foscari di Venezia, Dorsoduro 2137, 30123 Venezia, Italy

Received July 11, 2006. Revised Manuscript Received February 13, 2007

A new synthetic route for the deposition of $CoAl_2O_4$ thin films at low temperature via MOCVD using the single-source precursor $\{Co[Al(O^iC_3H_7)_4]_2\}$ is presented. Molecular properties of $\{Co[Al(O^iC_3H_7)_4]_2\}$ have been investigated by means of NMR spectroscopy, mass spectrometry, and thermal analysis. Deposits have been characterized by XRD, AFM, UV−vis, and SIMS measurements.

Introduction

Metal spinels (MAl_2O_4, where M = bivalent metal) represent an interesting class of materials having a wide range of applications.[1] Among MAl_2O_4, cobalt aluminate ($CoAl_2O_4$, the Thenard's blue) plays an important role in the sensor and semiconductor technology as well as in the field of heterogeneous catalysis, such as the CO_2 reforming of methane.[2] Moreover, its peculiar optical properties[3] make it very appreciated as pigment[4−6] and coating, e.g., in color filters and luminescence materials.[7−10] Even though $CoAl_2O_4$ is mainly prepared in the form of powder samples,[3,11−14] specific applications would require high-quality thin films whose preparation can be achieved only by means of nonconventional techniques. In relation to that, we mention that we recently reported the preparation of $CoAl_2O_4$ thin films through the MOCVD of the dual precursor system $[(C_5H_5)_2Co]$ and $[(CH_3)_2AlO^iC_3H_7]$.[15] In this contribution, we showed that, besides the need of the two precursors, $CoAl_2O_4$ deposits could be obtained only through a dual-step process involving the deposition of Co and Al oxides (former step), followed by their annealing in air at high temperature (800−1200 °C) for 12 h (latter step). In this regard, it is noteworthy that high-quality thin films may be prepared in milder conditions by adopting the sol−gel technique and using the single-source precursors $\{Co[Al(O^iC_3H_7)_4]_2\}$ or $\{Co[Al(OC(CH_3)_3)_4]_2\}$.[1,8,13,16] Such a knowledge prompted us to attempt the first MOCVD deposition of $CoAl_2O_4$ thin films by using $\{Co[Al(O^iC_3H_7)_4]_2\}$. Incidentally, it is of some relevance to point out that thin films of $MgAl_2O_4$ (a ternary oxide having the same structure of $CoAl_2O_4$) have been successfully chemical-vapor-deposited by related single-source precursors.[17−21]

Experimental Section

Precursor. All synthetic manipulations were carried out under an oxygen- and moisture-free atmosphere of a MBraun MB 200G-II drybox with an organic solvents scavenger. All ethereal and hydrocarbon solvents were dried and distilled before their use following standard procedures.[22] Anhydrous $CoCl_2$ has been

---

* To whom correspondence should be addressed. E-mail: zanella@icis.cnr.it (P.Z.); maurizio.casarin@unipd.it (M.C.). Phone: 39 049 8295941 (P.Z.); 39 049 8275164 (M.C.). Fax: 39 049 8702911 (P.Z.); 39 049 8275161 (M.C.).
† Istituto di Chimica Inorganica e delle Superfici.
§ Departmento di Fisica, Università degli Studi di Padova.
‡ Departmento di Scienze Chimiche, Università degli Studi di Padova.
|| Università Ca'Foscari di Venezia.

(1) Platero Escalona, E.; Otero Areán, C. O.; Parra, J. B. *Res. Chem. Intermed.* **1999**, *25*, 187.
(2) Ji, L.; Tang, S.; Zeng, H. C.; Lin, J.; Tan, K. L. *Appl. Catal., A* **2001**, *207*, 247.
(3) Stangar, U. L.; Orel, B.; Krajnc, M.; Korošec, R. C.; Bukovec, P. *Mater. Tehnol.* **2002**, *36*, 187.
(4) Buxbaum, G. *Industrial Inorganic Pigments*, 2nd ed.; Wiley−VCH: Weinheim, Germany, 1998.
(5) Minunno, G. *Azzurri in La Fabbrica dei Colori*; Bagatto Libri: Rome, 1995.
(6) Melo, D. M. A.; Cunha, J. D.; Fernandes, G. D. G.; Bernardi, M. I.; Melo, M. A. F.; Martinelli, A. E. *Mater. Res. Bull.* **2003**, *38*, 1559.
(7) Li, W.; Li, J.; Guo, J. *J. Eur. Ceram. Soc.* **2003**, *23*, 2289.
(8) Otero Areán, C. O.; Mentruit, M. P.; Platero, Escalona E.; Llbrés i Xamena, F. X.; Parra, J. B. *Mater. Lett.* **1999**, *39*, 22 and references therein.
(9) Merikhi, J.; Jungk, H. O.; Feldmann, C. J. *J. Mater. Chem.* **2000**, *10*, 1311.
(10) Stangar, U. L.; Orel, B.; Krajnc, M. J. *Sol−Gel Sci. Technol.* **2003**, *26*, 771.
(11) Schmidt, W.; Weidenthaler, C. *Chem. Mater.* **2001**, *13*, 607 and references therein.
(12) Zayat, M.; Levy, D. *Chem. Mater.* **2000**, *12*, 2763.
(13) Meyer, F.; Hempelmann, R.; Mathur, S.; Veith, M. *J. Mater. Chem.* **1999**, *9*, 1755.
(14) Cho, W. S.; Kakihana, M. J. *J. Alloys Compd.* **1999**, *287*, 87.
(15) Carta, G.; Casarin, M.; El Habra, N.; Natali, M.; Rossetto, G.; Sada, C.; Tondello, E.; Zanella, P. *Electrochim. Acta* **2005**, *50*, 4592.
(16) Meyer, F.; Dierstein, A.; Beck, C.; Härtl, W.; Hempelmann, R.; Mathur, S.; Veith, M. *Nanostruct. Mater.* **1999**, *12*, 71.
(17) Mathur, S.; Veith, M.; Ruegamer, T.; Hemmer, E.; Shen, H. *Chem. Mater.* **2004**, *16*, 1304.
(18) Koh, W.; Ku, S. J.; Kim, Y. *Chem. Vap. Deposition* **1998**, *4*, 192.
(19) Veith, M.; Altherr, A.; Wolfanger, H. *Chem. Vap. Deposition* **1999**, *5*, 87.
(20) Rocheleau, R. E.; Zhang, Z.; Gilje, J. W.; Meese-Marktscheffel, J. A. *Chem. Mater.* **1994**, *6*, 1615.
(21) Boo, J. H.; Lee, S. B.; Ku, S. J.; Koh, W.; Kim, C.; Yu, K. S.; Kim, Y. *Appl. Surf. Sci.* **2001**, *169−170*, 581.
(22) Perrin, D. D.; Armarego, W. L. F., Perrin, D. R. *Purification of Laboratory Chemicals*, 2nd ed.; Pergamon Press: Oxford, UK, 1980.

10.1021/cm0615931 CCC: $37.00

obtained by dehydration of $CoCl_2{\cdot}6H_2O$ refluxed with an excess of $(CH_3)_2SiCl_2$ at 70 °C for 5 h. It was then filtered, washed with $(CH_3)_2SiCl_2$, and dried in vacuo. $\{Co[Al(O^iC_3H_7)_4]_2\}$ was prepared according to the procedure published by Mehrotra et al.[23] Elemental analyses were performed using a FISON Instruments, model EA 1108 CHNS-O. The ^1H NMR spectra were recorded on a Bruker AMX-300 spectrometer operating at 300 MHz. EI mass spectra were recorded on a Finnigan Trace MS using a ThermoQuest direct-injection probe.

Controlled thermal analysis of the complex was investigated using a TA DSC 2920 instrument. The measurements were carried out in alumina crucibles under an atmosphere of flowing nitrogen gas.

Thin Film Deposition. Deposition experiments were performed in a horizontal hot wall LP-MOCVD reactor. Total pressure, gas-phase composition, and substrate temperature were adjusted independently. The precursor bubbler has been thermostated at 150 °C in an oil bath, whereas the gas tubing between the bubbler and the reactor furnace was maintained at 170 °C to avoid vapor condensation. The precursor vapor has been carried to the reactor by a 50 sccm N_2 flux. Thin films have been deposited in an oxidizing atmosphere bubbling O_2 (100 sccm) into a distilled H_2O vessel (at room temperature), and the resulting H_2O/O_2 mixture was introduced as reactant gas in contact with the precursor vapor in proximity of the substrates placed inside the furnace. The substrates were small rectangular flat pieces (1×1 cm^2) of Si-(100) and fused quartz, previously washed first with hot trichloroethylene (98%) and then rinsed with acetone. Depositions have been carried out at a total pressure of 1 Torr and at temperatures ranging between 350 and 700 °C with a reaction time of 45 min, using freshly prepared $\{Co[Al(O^iC_3H_7)_4]_2\}$ as precursor.

After film depositions, the samples were exposed to a thermal annealing at 500−800 °C in either air or a N_2 atmosphere.

Film Characterization. All samples have been characterized by UV−vis, XRD, AFM, EDX, and SIMS analyses. UV−vis spectra were recorded on a double beam UV500-spectrometer (Spectronic Unicam) based on Vision 32 software and operating in transmission mode (in the 250−900 nm range). The phase characterization was done by X-ray diffraction (XRD) measurements, performed on as-deposited and annealed films, by using a Philips PW1830 powder diffractometer in Bragg−Brentano geometry using Cu Kα radiation (40 kV, 30 mA, $\lambda = 1.54056$ Å). The detector was a Xe gas proportional counter equipped with a secondary curved graphite monochromator. The patterns were collected in the 25−70° 2θ range at grazing incidence ($\Omega = 2°$). Peak positions were determined with a statistical error of $d(2\theta) = 0.02°$. Phase identification was performed using standard spectra reported in the JCPDS database. The surface topology and the average roughness of the deposited films were performed with a DME Dualscope^{TM} atomic force microscopy (AFM) using silicon cantilever tips with a nominal tip radius of 10 nm, operating with tubular scanner and in noncontact mode.

Compositional analysis was carried out by a scanning electron microscopy (SEM) through a Philips XL-40 microscopy with a LaB_6 source. The instrument was equipped with an analytical system working in energy dispersion (EDS-EDAX DX PRIME).

Secondary ion mass spectrometry (SIMS) measurements were carried out by means of an IMS 4f mass spectrometer (Cameca) using a 10 kV Cs^+ primary beam and by negative secondary ion detection (the sample potential was fixed at −4.5 kV) with a final impact energy of 14.5 keV. SIMS spectra were carried out in ultra high vacuum (UHV) conditions at different primary beam intensity (50 nA) rastering over a nominally 125×125 μm^2 area. Beam blanking mode was used to improve the depth resolution, interrupting the sputtering process during magnet stabilization periods. The erosion speed was evaluated by measuring the depth of the erosion crater at the end of each analysis by means of a Tencor Alpha Step profilometer with a maximum uncertainty of few nanometers. The dependence of the erosion speed on the matrix composition was taken into account for each sample by measuring it at various depths. The measurements were performed in high mass resolution configuration to avoid mass interference artifacts. The charge build-up occurring in insulating samples during the in-depth profiling was compensated by an electron gun without any need to cover the surface with a metal film.

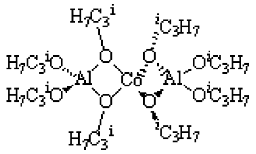

Figure 1. Structural formula of $\{Co[Al(O^iC_3H_7)_4]_2\}$ in benzene-d$_6$.

Results and Discussion

Precursor. The use of a single-source precursor for the deposition of multicomponent films via MOCVD requires the choice of a suitable compound characterized by a certain volatility. Our attention has been then focused on $\{Co[Al(O^iC_3H_7)_4]_2\}$, whose sublimation temperature is 140 °C at 0.6 Torr.[23]

According to the synthesis reported by Mehrotra,[23] the reaction of $[KAl(O^iC_3H_7)_4]$, prepared in situ from $K(O^iC_3H_7)$ and $Al(O^iC_3H_7)_3$, with $CoCl_2$ yields the heterobimetallic derivative $\{Co[Al(O^iC_3H_7)_4]_2\}$ (eq 1) as a violet viscous liquid.

$$Al(O^iC_3H_7)_3 \xrightarrow[-KCl]{\substack{+\,K[O^iC_3H_7] \\ +\,1/2\,CoCl_2}} Co[Al(O^iC_3H_7)_4]_2 \qquad (1)$$

To the best of our knowledge, the characterization of $\{Co[Al(O^iC_3H_7)_4]_2\}$ is limited to its elemental analysis;[23] to look into its chemical behavior, we investigated its properties by means of NMR spectroscopy, mass spectrometry, and thermal analysis.

The ^1H NMR spectrum in benzene-d$_6$ at room temperature presents two broad resonances at 97.8 ($\delta\nu_{1/2} = 822$ Hz) and −29.7 ppm ($\delta\nu_{1/2} = 1688$ Hz), which can be assigned to the methyl and methyne protons of the isopropyl groups, respectively (proton absorptions are strongly affected by the paramagnetic Co^{2+} center). Moreover, the two methyl ^1H resonances detected at 190 K in toluene-d$_8$ at −173 and 62 ppm coalesce at ca. 220 K. Therefore, the molecular structure of $\{Co[Al(O^iC_3H_7)_4]_2\}$ in benzene-d$_6$ should be analogous to that of the *tert*-butoxide derivative $\{Co[Al(OC(CH_3)_3)_4]_2\}$,[24,13] with bridging and terminal isopropoxide groups (see Figure 1).

Thermal behavior of $\{Co[Al(O^iC_3H_7)_4]_2\}$ has been studied via mass spectrometry and thermal analysis. Electron impact spectrum shows a series of mass peaks reported in Table 1. Molecular peaks ($m/z = 585$) occurs in reduced abundance

---

(23) Singh, J. V.; Jain, N. C.; Mehrotra, R. C. *Synth. React. Inorg. Metal−Org. Chem.* **1979**, *9*, 79.

(24) The exchange of the nonequivalent isopropoxide ligands yields the observed averaged spectrum at room temperature.

Table 1. Natural Abundance and *m/z* Ratio of the Mass Peaks Obtained from the EI Spectrum of $\{Co[Al(O^iC_3H_7)_4]_2\}$ Precursor.

species	*m/z*	natural abundance
$C_{24}H_{56}Al_2CoO_8]^{+\bullet}$ (M$]^{+\bullet}$)	585	3
$C_{22}H_{53}Al_2CoO_8]^{+}$	570	59.7
$C_{19}H_{43}Al_2CoO_8]^{+}$	512	19.8
$C_{18}H_{42}Al_2CoO_6]^{+\bullet}$	468	15.2
$C_{15}H_{33}Al_2CoO_8]^{+}$	454	50.5
$C_{15}H_{35}Al_2CoO_6]^{+}$	424	95.2
$C_{13}H_{29}Al_{l2}CoO_7]^{+}$	410	100
$C_{15}H_{35}AlCoO_5]^{+}$	381	12.5
$C_{12}H_{28}AlCoO_4]^{+}$	322	37.2

(3%). Most of the lower-mass ions of significant abundance reported in Table 1 contain the correct Co:Al (1:2) ratio, suggesting that the metal atoms are joined rather strongly through oxygen bridges and that the preferred elimination involves alkyl (CH_3,C_3H_7) or isopropoxy groups.

Thermal analysis has been carried out in a N_2 atmosphere and results are reported in Figure 2. Initially, a moderate weight loss of about 3% occurs in the range 30−200 °C, and the weight loss then becomes more intense up to 280 °C (∼80%); finally, the weight of the sample is reduced to 10−12% at 320 °C, remaining unchanged up to 700 °C. Concomitantly, three endothermic phenomena (at ∼240, 280, and 318 °C, respectively) are observed. It is reasonable to assume that the initial weight loss is due to the sublimation, and then to the dissociation of the complex according to the following steps

$$\{Co[Al(O^iC_3H_7)_4]_2\} \rightarrow Co(O^iC_3H_7)_2 + 2\ Al(O^iC_3H_7)_3$$

$$Co(O^iC_3H_7)_2 \rightarrow Co + 2{\bullet}O^iC_3H_7$$

$Al(O^iC_3H_7)_3$ is a volatile molecule that evaporates completely at 200−250 °C, whereas $Co(O^iC_3H_7)_2$ thermally decomposes in the 280−320 °C temperature range. The residual solid corresponding to ca. 10% of the initial weight probably consists of metallic Co (∼10% of $\{Co[Al(O^iC_3H_7)_4]_2\}$). As a whole, these data demonstrate that $\{Co[Al(O^iC_3H_7)_4]_2\}$ is volatile and stable in a N_2 atmosphere up to 200 °C, thus indicating that the vaporized precursor can be carried unreacted to the CVD reactor below 200 °C. Before going on, it has to be emphasized that the deposition of $CoAl_2O_4$ films from $\{Co[Al(O^iC_3H_7)_4]_2\}$ needs the presence of O_2/H_2O. As matter of fact, thermogravimetric experiments carried out in air left a residue corresponding to a percentage sligtly less than the 30% of the initial weight, as expected for the formation of $CoAl_2O_4$ from the decomposition of $\{Co[Al(O^iC_3H_7)_4]_2\}$. It is noteworthy that any attempt to obtain $CoAl_2O_4$ films from $\{Co[Al(O^iC_3H_7)_4]_2\}$ in a N_2 atmosphere did not succeed, thus indicating that their deposition require the addition of suitable oxygenating co-reagents in the reaction chamber.

Thin Film Deposition. The film deposition has been carried out on substrates heated in the 350−700 °C temperature range. The Co:Al ratio determined by EDX analysis is 1:2. The deposition temperature is found to have a great influence on the optical and structural properties of the deposited layers. As a matter of fact, films obtained in the 350−550 °C temperature range were blue and amorphous, whereas those deposited at higher temperature (600−700 °C) were olive green and crystalline. Blue amorphous layers grown at 350−550 °C become green and polycrystalline when annealed in air above 500 °C. At variance to that, the annealing of the same layers in N_2 does not induce any color variation and the blue color persists even above 500 °C (crystallization takes place at 700 °C). Further thermal treatments of green films in air above 700 °C always turn their color to blue. Finally, after crystallization in air at 800 °C, blue films reheated in air from room temperature to 700 °C maintain their blue color. Before going on, it deserves to be remarked that analogous color changes induced by thermal treatments have been observed by several authors.[3,10,12−13]

The UV−vis spectra of the deposited films are displayed in Figures 3 and 4. All spectra show a structured absorption band ranging from ∼500 to ∼700 nm, with maxima at ca. 540, 585, and 630 nm. According to literature data,[25−32] this absorption feature is readily associated with the ν_3 ($^4A_2 \rightarrow {}^4T_1(P)$] ligand field band characteristic of the pseudo-tetrahedral Co^{2+} species.[33] In this regard, it has to be noted that different mechanisms may contribute to the determination of the shape of this band: (i) vibronic coupling; (ii) at first order, spin−orbit coupling ($\zeta_{Co2+\ \mathrm{free\ ion}} = 515\ cm^{-1}$)[34] splits tetrahedral ^4T states into three spinor components; (iii) the $^4T_1(P)$ state is expected to be quite close to doublet states deriving from the ^2G free-ion term,[32] and a significant spin−orbit mixing of quartet and doublet levels would relax the spinforbidness of transitions to formally doublet excited states. In this regard, it is worthwhile to mention that absorption spectra collected by Radovanovic and Gamelin[31] at 300 and 15 K for Co^{2+}-doped CdS indicated that, besides vibronic contributions, an important role in determining the structure of the band corresponding to the $^4A_2 \rightarrow {}^4T_1(P)$ excitation is played by spin−orbit coupling effects. In addition to the above bands, the UV−vis spectra of green colored samples are also characterized by the presence of a shoulder in the 350−450 nm range (Figure 3b and Figure 4a) which disappears when samples, appropriately annealed, became blue (Figure 4c).

It is well-known that blue materials absorb visible light in the 500−700 nm range, and that the green color is usually associated with a shoulder in the absorption spectrum lying at about 400 nm. Stangar et al.[10] claimed that such a shoulder is indicative of the presence of octahedral coordinated Co^{3+}

---

(25) Cotton, F. A.; Goodgame, D. M. L.; Goodgame, M. J. *J. Am. Chem. Soc.* **1961**, *83*, 4690.

(26) Belova, I. D.; Roginskaya, Y. E.; Shifrina, R. R.; Gagarin, S. G.; Plekhanov, Y. V.; Venevtsev, Y. N. *Solid State Commun.* **1983**, *47*, 577.

(27) Lever, A. B. P. *Inorganic Electronic Spectroscopy*, 2nd ed.; Elsevier Science Publisher: Amsterdam, The Netherlands, 1984; references therein.

(28) Martens, J. W. D.; Peeters, W. L.; Van Noort, M.; Erman, M. J. *J. Phys. Chem. Solids* **1985**, *46*, 411.

(29) Cook, J. G.; Van Der Meer, M. P. *Thin Solids Films* **1986**, *144*, 1654.

(30) Lenglet, M.; Jorgensen, C. K. *Chem. Phys. Lett.* **1994**, *229*, 616.

(31) Radovanovic, P. V.; Gamelin, D. R. J. *J. Am. Chem. Soc.* **2001**, *123*, 12207.

(32) Duan, X.; Yuan, D.; Cheng, X.; Sun, Z.; Sun, H.; Xu, D.; Lv, M. *J. Phys. Chem. Solids* **2003**, *64*, 1021.

(33) According to the Lever notation,[27] ν_1, ν_2, and ν_3 correspond to the $^4A_2 \rightarrow {}^4T_2$, $^4A_2 \rightarrow {}^4T_1(F)$, and $^4A_2 \rightarrow {}^4T_1(P)$ transitions, respectively, of a d^7 ion in a field of tetrahedral symmetry.

(34) Figgis, B. N. I*ntroduction to Ligand Fields*; Interscience Publishers: New York, 1967.

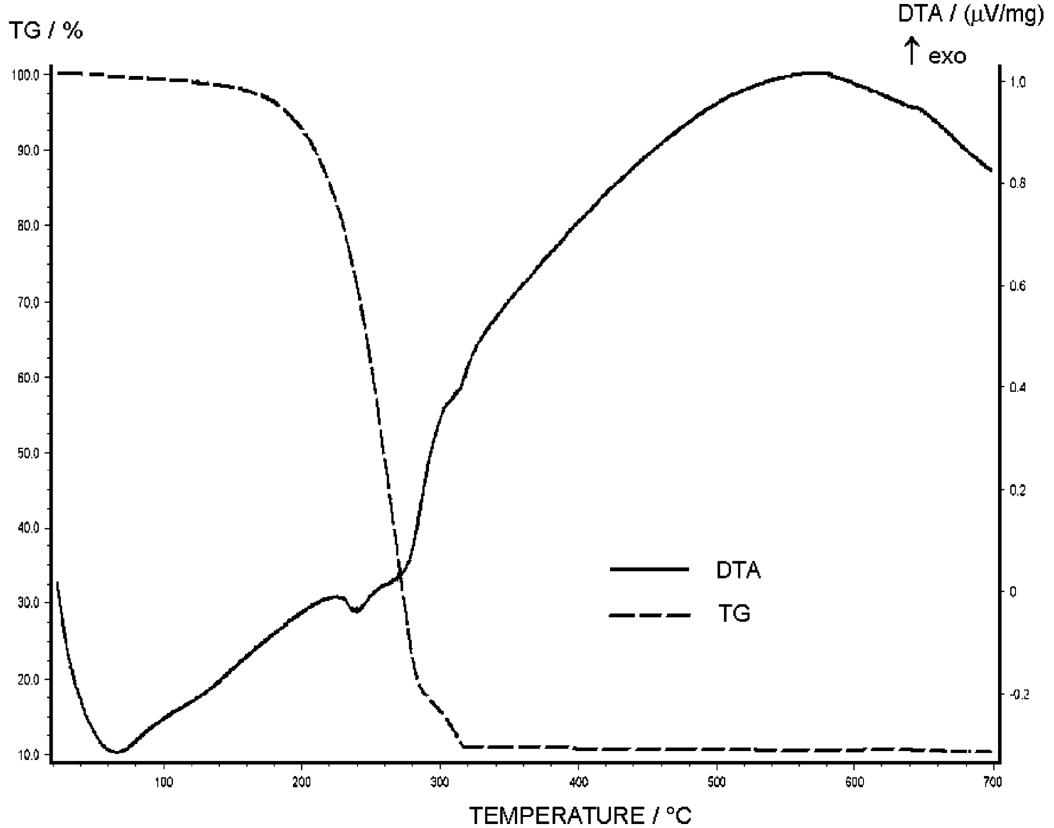

Figure 2. TGA-DTA profiles of $\{Co[Al(O^iC_3H_7)_4]_2\}$ precursor carried out in a N_2 atmosphere.

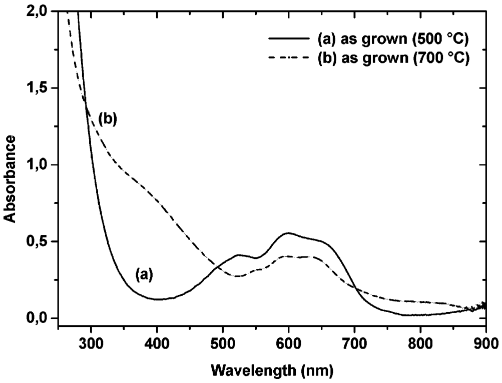

Figure 3. UV−vis absorbance spectra of the samples grown on fused-quartz at (a) 500 and (b) 700 °C.

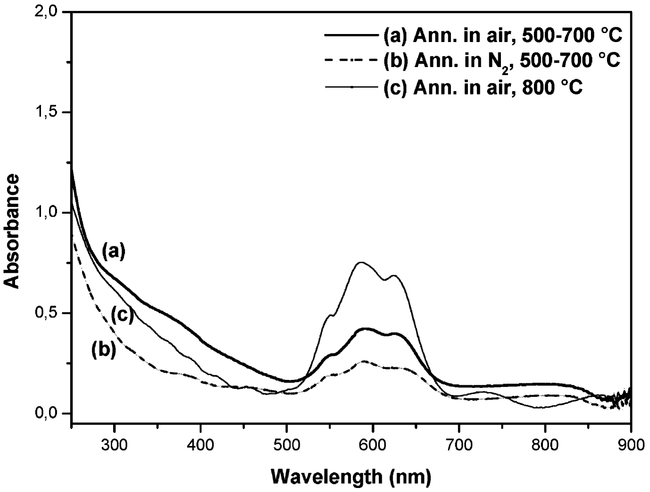

Figure 4. UV−vis absorbance spectra of the sample grown at 500 °C on fused-quartz and annealed (a) in air at 500−700 °C, (b) in N_2 at 500−700 °C, and (c) in air at 800 °C.

ions, even if the occurrence of the octahedrally coordinated Co^{2+} species (inverse spinel) cannot be ruled out.[35−36] Incidentally, it can be useful to remind that it is unanimously accepted that in mixed Co−Al oxides, Co^{2+} can be oxidized in air to Co^{3+} at 400−500 °C and can be reduced again to Co^{2+} at $T > 700$ °C, depending on the system composition.[3,10,12]

Besides the different color of samples grown at 350−550 °C (blue) and 600−700 °C (green), XRD spectra indicate that the former deposits are amorphous, whereas the latter are polycrystalline (Figure 5). Moreover, the annealing in air of the amorphous samples at 500 °C or at higher temperature promotes crystallization. Polycrystalline deposits are all characterized by rather similar diffraction patterns with well-shaped and rather narrow peaks in the 25−70° 2θ range. Furthermore, both the relative intensities of XRD reflections ($I_{220}/I_{311} = 0.65$) and the presence of a weak peak at $2\theta = 48.9°$ ($I_{331}/I_{311} = 0.04$) in blue films annealed above 700 °C (Figure 5e) ultimately indicate that they correspond to $CoAl_2O_4$ deposits.[37] XRD spectra of the blue samples annealed either in air above 700 °C or in N_2 at 500−700 °C (plots d and e in Figure 5) are rather similar; actually, the I_{220}/I_{311} ratio of the latter is 0.62, thus indicating akin

---

(35) Cava, S.; Tebcherani, S. M.; Pianaro, S. A.; Paskocimas, C. A.; Longo, E.; Varela, J. A. *Mater. Chem. Phys.* **2006**, *97*, 102.

(36) To settle this matter, a series of EXAFS measurements are in progress at the General purpose Italian beam Line for Diffraction and Absorption (GILDA) of the European Synchrotron Radiation Facility.

(37) The XRD peak at $2\theta = 48.9°$ can be ascribed to the (331) reflection of the $CoAl_2O_4$ spinel structure (JCPDS 44-0160).[3,10,12]

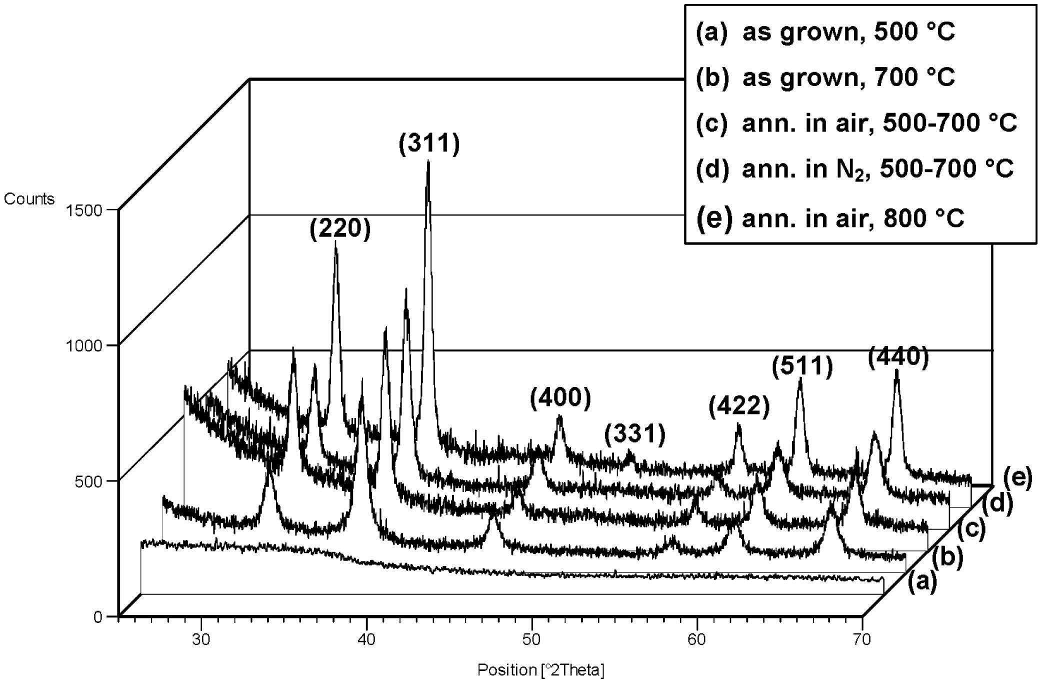

Figure 5. XRD profiles of the as-grown sample deposited (a) at 500 °C, (b) at 700 °C on fused-quartz and after annealing treatment (c) in air at 500−700 °C, (d) in N_2 at 500−700 °C, and (e) in air at 800 °C (for $CoAl_2O_4$: JCPDS 44-0160 with lattice size of 8.104 Å).

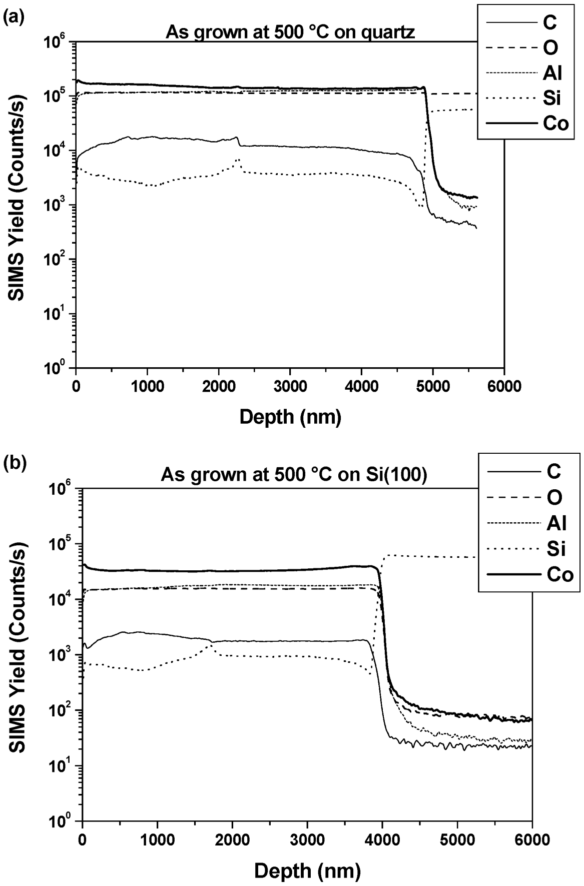

Figure 6. SIMS in-depth profiles of the as-grown sample at 500 °C on (a) fused-quartz and (b) Si(100).

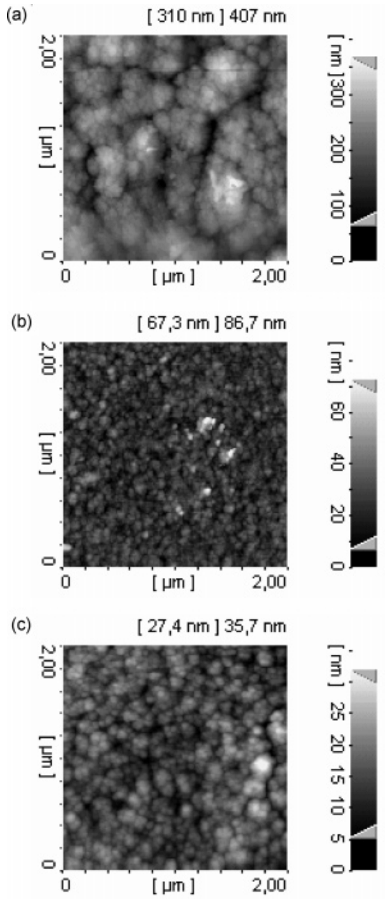

Figure 7. AFM micrographs (a) of the as-grown films deposited on Si-(100) at 500 °C and after annealing treatment in air at (b) 500 and (c) 800 °C.

composition. In this regard, it can be useful to point out that the low intensity of the whole diffraction pattern of samples annealed in N_2 avoids the detection of the weak peak at $2\theta = 48.9°$.

As far as the XRD spectra of polycrystalline green films are concerned, it has to be remarked that: (i) their XRD patterns are rather close to those of blue samples (see Figure 5); (ii) their color does not allow us to exclude the coexistence of $CoAl_2O_4$ and Co_2AlO_4 spinels, both having the same space group (*Fd*3*m*), very close unit-cell constants

(8.104 and 8.086 Å, respectively) and very similar XRD patterns (JCPDS 44-0160 and JCPDS 38-0814, respectively);[12] (iii) the I_{220}/I_{311} ratio of green samples (0.47 and 0.80 in plots b and c of Figure 5, respectively) differs from values pertaining to $CoAl_2O_4$ (0.65) and Co_2AlO_4 (0.35); (iv) preferential orientation could play a relevant role in determining different relative intensity values.

SIMS profiles of films grown on Si(100) and fused quartz are reported in Figure 6. Experimental outcomes reveal the presence of some carbon contamination persisting even after annealing; however, the Co, Al, and O profiles are characterized by a uniform trend all along the thickness of the layer, thus evidencing a very high compositional homogeneity. Moreover, the sharpness of the interface is indicative of a negligible interdiffusion. Film thickness ranges between ∼3.5 (∼2.6) and ∼5.0 (∼4.0) μm for deposits on fused quartz (Si) after 1 h growth. Such growth rates are quite relevant, even if their reproducibility is strongly affected by the high sensitivity of the precursor, which undergoes a partial decomposition if the deposition process is not strictly controlled.

AFM micrographs of the as grown films at 500 °C on Si(100) and after annealing in air at 500 and 800 °C are reported in Figure 7. The as-grown sample shows a double-scale roughness (Figure 7a) composed of large mounds covered by small grains having mean dimensions of 80 nm. Interestingly, the annealing treatment concomitantly favors the disappearance of mounds and the decrease in surface roughness (the root-mean-square roughness of the films changes from 43 nm for the as-grown sample to 7 and 4 nm after their annealing at 500 and 800 °C, respectively).

Conclusion

The complex $\{Co[Al(O^iC_3H_7)_4]_2\}$, a heterobimetallic alkoxide already described by Mehrotra, has been tested for the first time as single-source precursor for the vapor-phase deposition of thin films of $CoAl_2O_4$. $\{Co[Al(O^iC_3H_7)_4]_2\}$ is characterized by a significant volatility in the 100−150 °C temperature range at about 1 Torr pressure, and high deposition rates may be achieved. In comparison with the growth process based on dual-source precursor systems it is noteworthy to observe that the films obtained by using $\{Co[Al(O^iC_3H_7)_4]_2\}$ are characterized by: (i) a better control of the stoichiometry (Co:Al ratio); (ii) a higher phase purity; and (iii) a significantly lower deposition temperature (350 vs 1000 °C), thus allowing the use of thermal sensitive substrates. Deposits obtained in the 350−550 °C range appear amorphous, but their annealing in air between 500 and 700 °C induces crystallization and a color change to green. At variance to that, the annealing in N_2 does not originate any color variations and crystallization takes place at 700 °C. Green and blue crystalline samples present very similar X-ray diffraction patterns but different UV−vis spectra. Nevertheless, a thermal treatment above 700 °C produces blue, stable, and polycrystalline $CoAl_2O_4$ films.

Acknowledgment. The authors gratefully thank Carla Marega of the Dipartimento di Scienze Chimiche, Università di Padova, for the helpful discussions concerning the assignment of XRD spectra.

CM0615931